

# Microstructure of a plasma-sprayed superalloy coating/substrate

ANN M. RITTER, MICHAEL F. HENRY

*General Electric Company, Corporate Research and Development, Schenectady, New York 12301, USA*

Five different specimen preparation techniques were employed to characterize the microstructure of a cross-section of plasma-sprayed Rene' 125 coating on a Rene' 125 turbine blade substrate. These methods included optical microscopy, and transmission electron microscopy on three types of replicas and on thin foils. Interface and matrix precipitates were indentified using electron diffraction and energy dispersive spectrometry, with  $\text{HfO}_2$  and  $(\text{Hf, Zr})\text{O}_2$  the predominant phases at the coating/blade interface, and both  $(\text{Ti, Ta})\text{C}$  and  $\text{HfO}_2$  present in the coating. Those blade precipitates examined contained Hf and Ta, with some Ti and a little Co. A unique dendritic structure of  $\gamma'$  was also found intermittently along the interface. The combination of the five techniques provides a wide variety of information, and is a strong tool for characterizing complex microstructures.

## 1. Background

Microstructural studies of superalloys have often relied on the transmission electron microscope (TEM) to elucidate features beyond the resolution of light optical instruments. A frequently used type of sample is the two-stage, platinum-shadowed replica [1] of metallographically polished and etched surfaces. Information obtained from such replicas can be related both to light optical images and to micrographs from thin foils [2, 3]. In addition, the microstructural data can be a valuable supplement to phase identification by X-ray diffraction on extracted residues [4, 5]. With the advent of the scanning electron microscope (SEM), qualitative identification of phases on surfaces could be easily obtained [6, 7]. The secondary electron images themselves, however, are often of poor contrast, except when a heavy etch is employed [8]. For lightly etched samples, the SEM images are of lower resolution than are transmission electron micrographs of replicas from the same surface [9]. Extraction replicas, however, combine the higher resolution of the TEM with one of the advantages of the SEM, i.e. the ability to obtain compositional data from phases in their original place in the microstructure. Extraction replicas have been used in the examination of

superalloys, but probably not as extensively as on low alloy and stainless steels. This is perhaps due to the usually coarser grain size of the superalloys, and the larger dimensions of the phases themselves. Extraction replication works best on precipitates roughly  $\leq 1 \mu\text{m}$  in size. The technique has been used to evaluate the morphology of such small phases as  $\gamma'$  in the matrix [10] and various compounds on grain boundaries, and to compare the data with those obtained from thin foils and from shadowed replicas [11, 12]. Indeed, as the size of general microstructural features decreases, efforts involving optical microscopy, SEM, and TEM/STEM of thin foils and extraction replicas provide fairly comprehensive information on microstructure and on phase identities. This trend is most evident in research on superalloy powders, which have been extensively characterized with the methods described above [13–15]. Therefore, since the microstructural constituents of plasma-sprayed coatings might be expected to be on a fine scale, the present investigation considers the types of information obtainable on such a coating with a combination of optical microscopy and three different replication techniques, and correlates the results with data from TEM of thin foils.

## 2. Experimental procedure

The specimen chosen was a cast jet engine turbine blade which had been coated using high-energy, low-pressure plasma spray. The substrate and coating compositions were both René 125 (nominally Ni-10.0 Co-8.9 Cr-7.0 W-4.75 Al-3.8 Ta-2.5 Ti-2.0 Mo-1.5 Hf-0.11 C-0.05 Zr-0.01B). The cross-section mounted and polished was along the axis of the blade at a segment near the platform. Examination was limited to the substrate/coating region at the top of the blade platform, and five different specimen preparation techniques were used.

The sample was electrolytically etched in a

solution of 10 ml  $H_3PO_4$  in 100 ml water, and the platform region was replicated using a standard acetylcellulose tape/Pt shadow/carbon deposition method [1]. The sample was repolished, etched for 15 sec in a 10% bromine/90% methanol solution, and an extraction replica then made from this surface, using an acetylcellulose tape/carbon deposition method described elsewhere [14]. Once the extraction replica had been made, optical microscopy was done on the bromine-etched sample. A portion of the carbon-coated acetylcellulose tape containing the extracted precipitates was also shadowed with Pt to enhance the microstructural features, and a replica sample made from this.

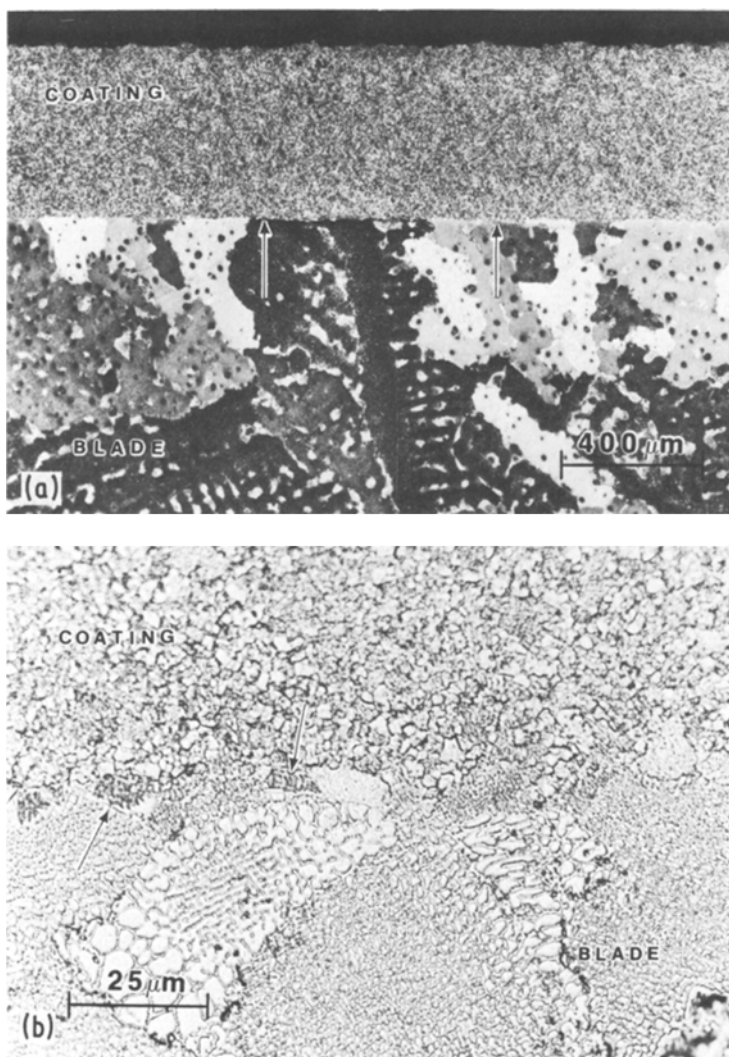


*Figure 1* René 125 blade and plasma-sprayed coating: (a) an optical micrograph (Condition C) shows apparent cleanliness and continuity of the interface (arrows), and (b) small regions containing fine dendrites (arrows), which also are observed (c) on the replica (Condition A), and are designated by arrows.

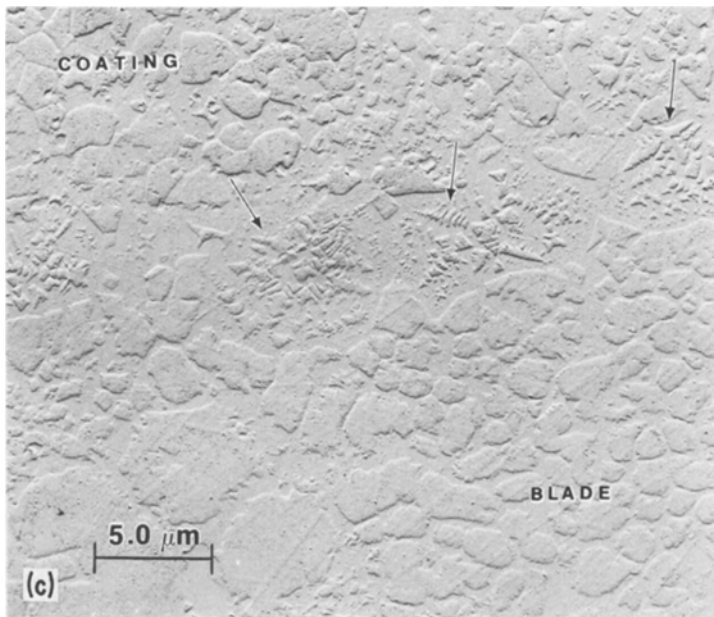


Figure 1 continued.

Thin foils were made from a section cut parallel to the surface examined by optical and replica methods. The slice was ground to about 0.10 mm thick, and pieces 3 mm long were cut from this. The pieces included both coating and blade regions. Platinum apertures were used during the electrothinning, in order to position the coating/blade interface at the centre of the polishing fixture. One foil thinned through the coating, one in the blade, and the last piece thinned at the interface. The electropolishing was done using a Fischione twin-jet apparatus, operated at 30 V. The solution was 20% perchloric acid/80% methanol at a temperature of  $-40^{\circ}\text{C}$ .

The five specimen conditions can be summarized as:

Condition	Description
A	Pt-replica, phosphoric acid etch
B	Extraction replica, Br-etch
C	Optical microscopy, Br-etch
D	Pt-replica, Br-etch
E	Thin foils

The replicas and foils were examined using a Hitachi H600 transmission electron microscope (TEM) and a JEOL JSEM-200 scanning-transmission electron microscope (STEM). Energy dispersive X-ray spectra were taken from extraction replicas using the JEOL STEM, which is equipped with a

Nuclear Semiconductor energy dispersive spectrometer (EDS) and a Tracor Northern NS880 analyser with a PDP11 computer.

### 3. Results and discussion

Examination of optical micrographs at lower magnification shows a clear demarcation between the plasma spray (PS) coating and the blade (Fig. 1a). The true structure of the interface is unclear at intermediate magnifications ( $\times 300$ ), although at  $\times 1200$  what appear to be very small regions of finely spaced dendrites are visible in some interfacial regions (Fig. 1b). Precipitation at the interface is not resolvable at this magnification with light optical microscopy.

The Pt-shadowed replicas of the phosphoric acid etched sample illustrate some of the fine interfacial structure fairly clearly. Precipitation in that area is difficult to see, but those areas which appeared optically to contain small dendrites are well resolved by the replica (Fig. 1c). The matrix near the small dendrites does not seem to contain blocky  $\gamma'$  ( $\text{Ni}_3\text{Al}$ ), seen in the adjacent coating, and there is a fine background structure which might be quench  $\gamma'$ . The interfacial dendrites themselves etch like  $\gamma'$ , or possibly beta ( $\text{NiAl}$ ), but positive identification of this phase is not possible by replication.

Precipitation other than  $\gamma'$  is observed using

extraction replication, which shows a line of small precipitates at the blade/coating interface (Fig. 2a). These range from 0.03–0.2  $\mu\text{m}$  in size. The contrast of the extraction replica is low, since it consists only of a layer of carbon with no shadowing material. Thus, it is difficult to relate precipitate distribution to general microstructural features. This problem was overcome by Pt-

shadowing the extraction replica. One sees from the micrographs of the interface that most of the regions containing the small dendrites appear to lie on the blade side of the line of precipitates (Fig. 2b), although these regions do extend into the coating to a limited degree. This observation tends to support the possibility of some incipient melting on the substrate of the thin platform

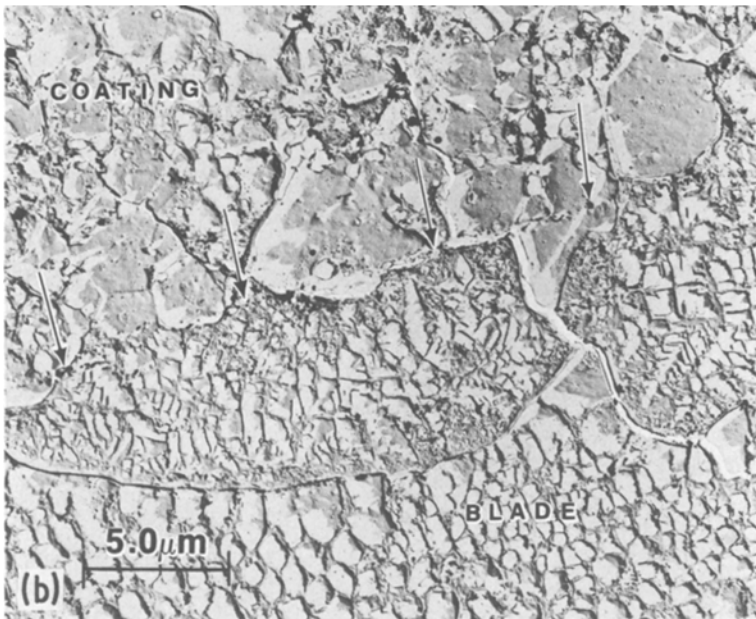
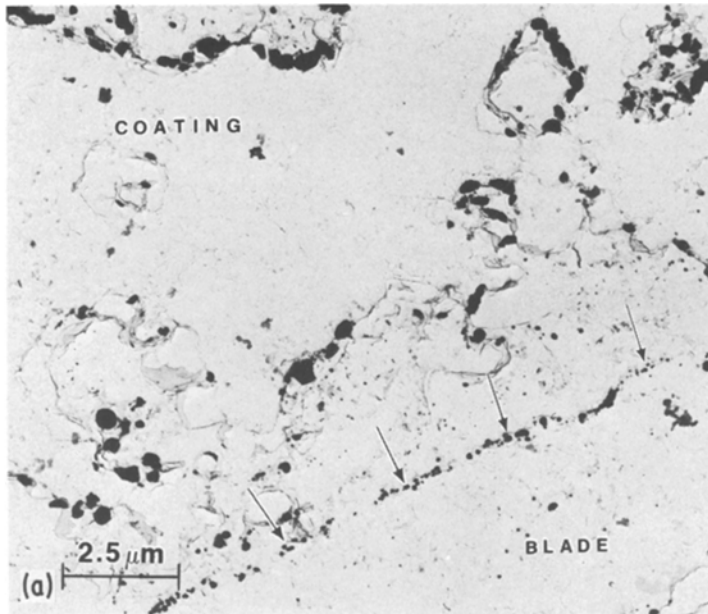


*Figure 2* Interfacial precipitates are seen (a) on the extraction replica (Condition B), and (b) the Pt-shadowed extraction replica (Condition D). Note that dendrites lie primarily on the blade side of interfacial precipitates (arrows). An EDS spectrum (c) from small interface precipitates finds them rich in Hf, occasionally with some Zr.

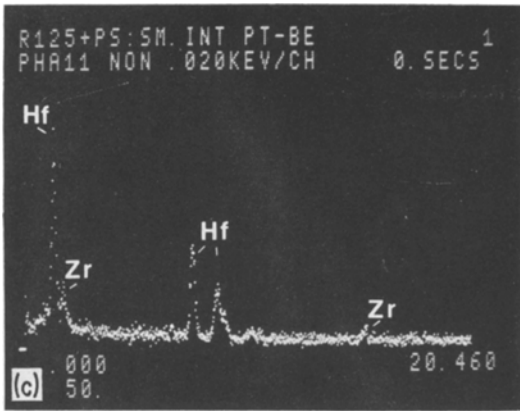


Figure 2 continued.

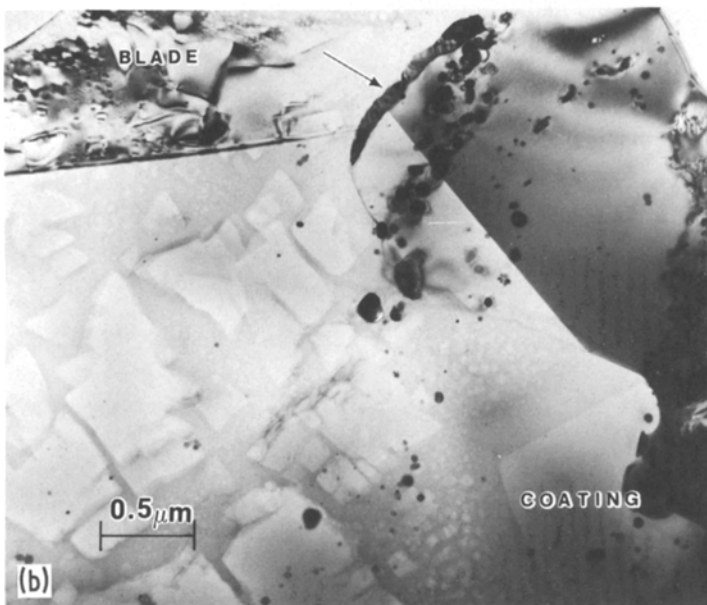
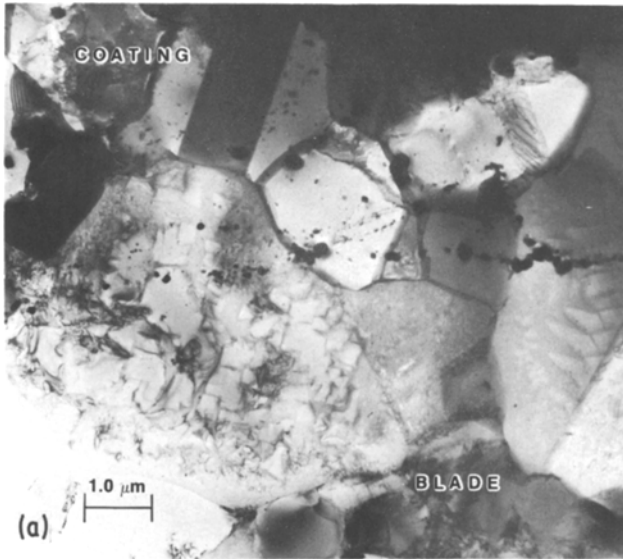
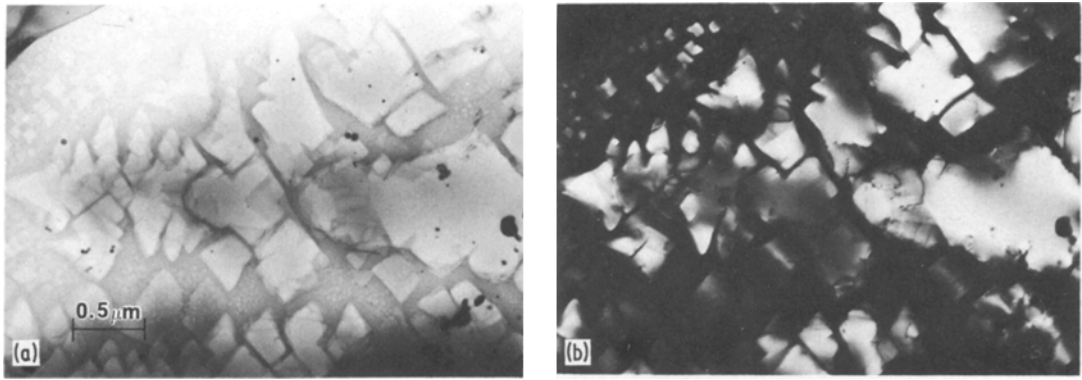
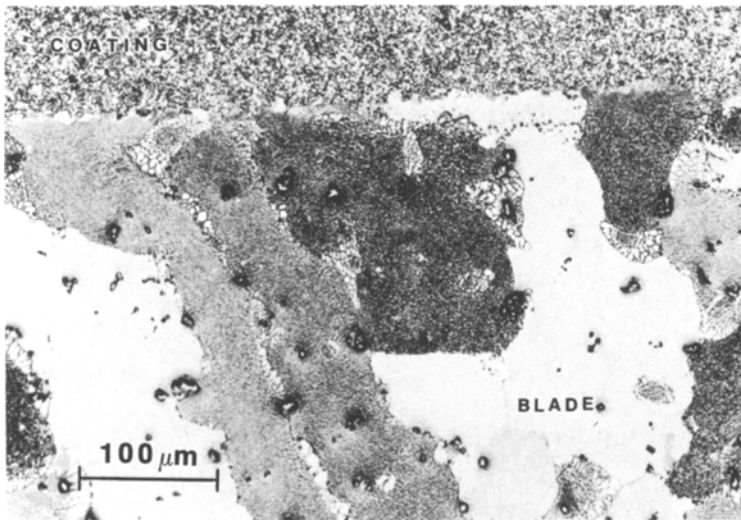


Figure 3 A thin foil (Condition E) from interface regions shows (a) a line of  $\text{HfO}_2$  precipitates associated with the interface, as well as  $\gamma'$  dendrites (b) in the melted regions. The small precipitates in the matrix around the dendrites are also  $\gamma'$ . A grain boundary is indicated by arrows.



*Figure 4* Dendrites in the melted region appear in (a) the bright-field TEM image of the thin foil, and (b) the dark-field image formed using a (110)  $\gamma'$  superlattice spot. Dendrites and fine  $\gamma'$  precipitates all have the same orientation with respect to the matrix.



*Figure 5* An optical micrograph (Condition C) of coating and blade, showing large grains in the latter.

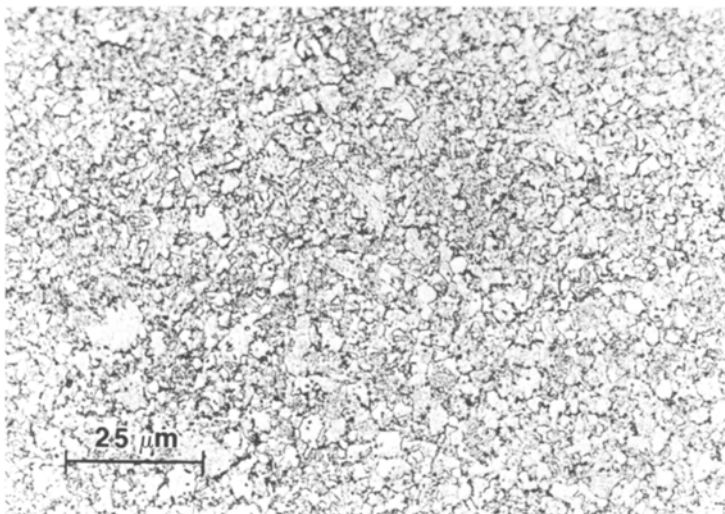


*Figure 6* Grains in the coating are observed optically at high magnification (Condition C).

before coating started, but could also be due to some incipient melting at onset of impact of the sprayed particles.

In order to obtain information on the chemistry of the precipitates, energy dispersive X-ray spectra (EDS) were taken on extracted precipitates on the carbon-only replica. Owing to the suspected presence of Hf, a special replica was prepared using a Be grid, as the X-rays emitted by Be are not

detectable by the spectrometer. This was done because the primary *L*-lines of Hf are close to the *K*-lines of Cu, the standard grid material, while the Hf *M*-line is near the *K*-lines of Al, a possible component in the precipitates. The small precipitates at the interface are found by this method to be Hf-rich, with some Zr in a few of them (Fig. 2c). This elemental analysis represents the qualitative composition of the phases, exclusive of any light

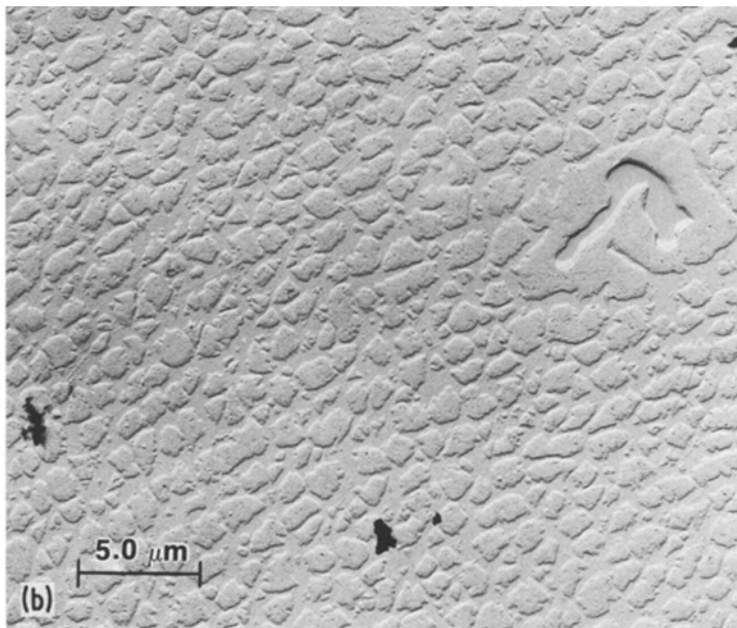
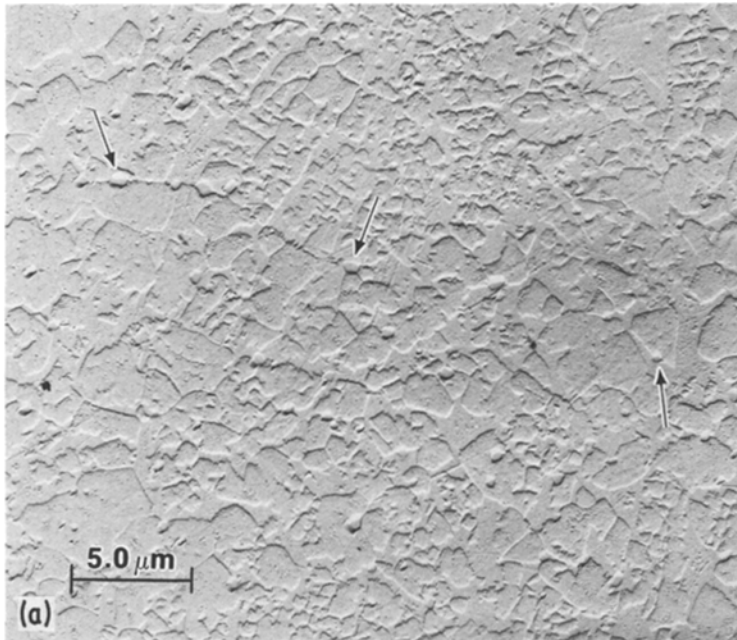
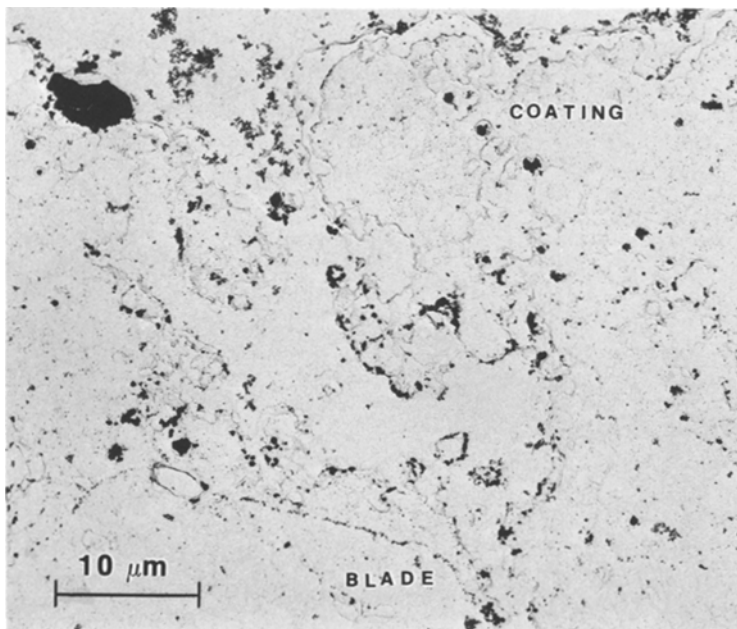


Figure 7 A replica (Condition A) shows (a) large blocky  $\gamma'$  in coating and small precipitates (arrows), which exhibit reverse contrast from  $\gamma'$ , and (b) large  $\gamma'$  in the blade somewhat more regular in shape than the  $\gamma'$  in the coating.





*Figure 8* An extraction replica (Condition B) best illustrates the distribution of coating precipitates, which are of widely varying sizes. The different densities of extracted precipitates may represent differing responses of regions to the etchant.

elements (less than atomic number 11), and illustrates one of the main advantages of extraction replicas over thin foils in phase chemistry determination, i.e. that spectra obtained on the replicas do not contain peaks from surrounding matrix. In thin foils, such peaks arise if the precipitate is of a size less than the effective area of the electron beam, or if the generation of X-rays in the precipitate causes fluorescence of elements in the matrix.

Selected-area electron diffraction patterns were obtained from the interfacial precipitates in order to identify them conclusively. The patterns were analysed as  $\text{HfO}_2$ , with a monoclinic structure (J.C.P.D.S. Powder Diffraction File No. 6-0318), and lattice parameters of  $a = 0.512 \text{ nm}$ ,  $b = 0.518 \text{ nm}$  and  $c = 0.522 \text{ nm}$ , with the angle  $\beta = 98.0^\circ$ . Since  $\text{ZrO}_2$  can also be monoclinic with similar lattice parameters and angles, the presence of a small amount of Zr, detected by EDS, in some of the primarily Hf-rich precipitates is consistent with the crystal structures of both  $\text{HfO}_2$  and  $\text{ZrO}_2$ .

Examination of the portion of coating/blade interface in the thin foil shows microstructural features seen in the various replicas. Regions containing dendrites lie primarily on the blade side of the interface, which is delineated by fine  $\text{HfO}_2$  precipitates (Fig. 3a). At higher magnifications, details suggested by the replicas, e.g. fine  $\gamma'$  between the dendrites, are very clear in the thin foil (Fig. 3b). In addition, it is possible to cor-

roborate the tentative identification of the dendrites as  $\gamma'$  by selected-area electron diffraction. This is illustrated by the bright-field/dark-field pair in Fig. 4. Dendrites and fine  $\gamma'$  seen in the bright-field image (Fig. 4a) appear light in the dark-field micrograph (Fig. 4b), imaged using a (110)  $\gamma'$  superlattice reflection. All  $\gamma'$  in the melted region has the same orientation relative to the matrix, and may have formed by a eutectic transformation.

The characterization methods described above were also applied to the coating and blade in order to define and compare the microstructures. At intermediate magnifications in the optical microscope, as in Fig. 5 at  $\times 300$ , individual features in the blade, such as large precipitates (presumably MC carbides) and eutectic regions, are apparent. At this same magnification, discreet grains in the more rapidly solidified coating are not resolved, as the microstructure is very fine. Observation at  $\times 750$ – $1200$  does show the grains in the coating (Fig. 6).

Examination of the Pt-shadowed replicas indicates that the intermediate size  $\gamma'$  in the coating (Fig. 7a) tends to be somewhat larger and more irregular than that in the blade (Fig. 7b). Fine  $\gamma'$  is not generally seen between the intermediate  $\gamma'$ , perhaps due to insufficient etching. It is interesting to note, that although individual grains in the coating can be resolved optically, grain boundaries



are not seen in the replicas. This is probably due to an insufficient etching differential between grain and grain boundary. In the blade, however, where grain boundaries often contain eutectic substructure, the boundaries are well defined.

Small rounded precipitates, which are observed optically at high magnifications, are seen in the replicas of the coating and show reverse shadowing contrast from the  $\gamma'$  (Fig. 7a). This indicates that the precipitates were relatively unaffected by the

etchant. The larger of these phases are approximately  $0.5\ \mu\text{m}$  and the smaller  $0.2\ \mu\text{m}$ . Such precipitates are not seen as frequently in the blade, but the general distribution of the non- $\gamma'$  phases is best studied by extraction replication of etched surfaces.

Extraction replication does show numerous precipitates in the coating (Fig. 8), and illustrates the various sizes present, from  $0.03\text{--}0.5\ \mu\text{m}$ , the smallest of which were not detected in the Pt-

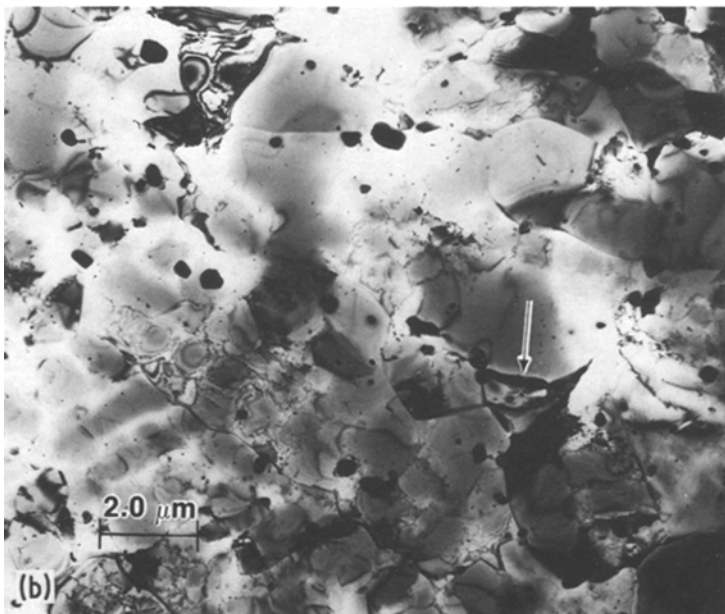
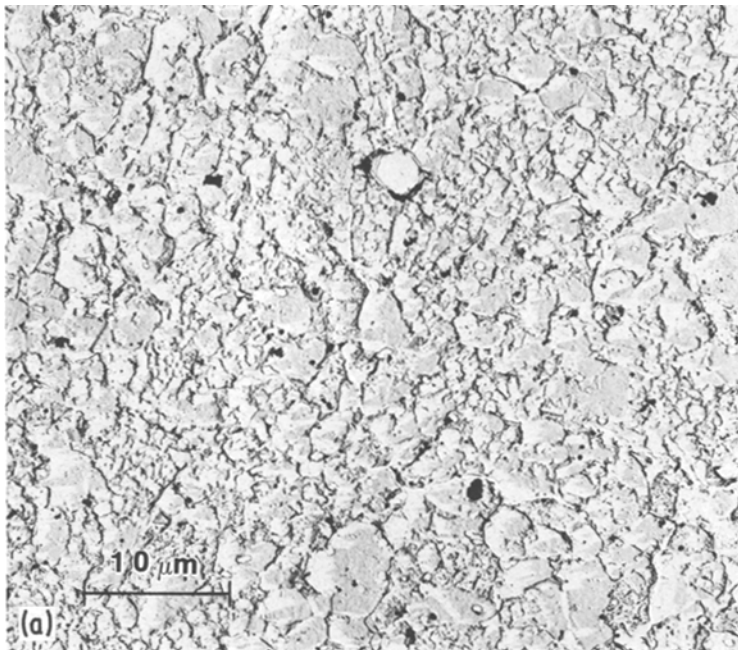


*Figure 9* Even distribution of precipitates relative to  $\gamma'$  in coating appears in (a) Pt-shadowed replica (Condition D), and (b) thin foil (Condition E). A grain-boundary phase (arrow) is also in this field of view.

shadowed replicas. The coating also shows some inhomogeneity in structure, as represented by the different etching rates from area to area. Clusters of large precipitates are observed, and may indicate sites of porosity in the coating. In the same micrograph are regions which did not etch well, and in which the number of extracted precipitates is small. In an area in which the extracted particles are more evenly dispersed, the precipitates also appear to be evenly distributed relative to the other microstructural features, such as  $\gamma'$ . This can

be seen in the Pt-shadowed extraction replicas (Fig. 9a), taken in regions which do not contain large clumps of precipitates. Areas of homogeneous precipitate distribution are present in the thin foils (Fig. 9b). In addition to those intragranular phases observed on the extraction replicas, precipitates associated with the grain boundaries are seen in the foils. That these were not extracted points out the occasional selectivity of the extraction replica technique, which relies on a combination of etching the matrix adjacent to the phases, and relative

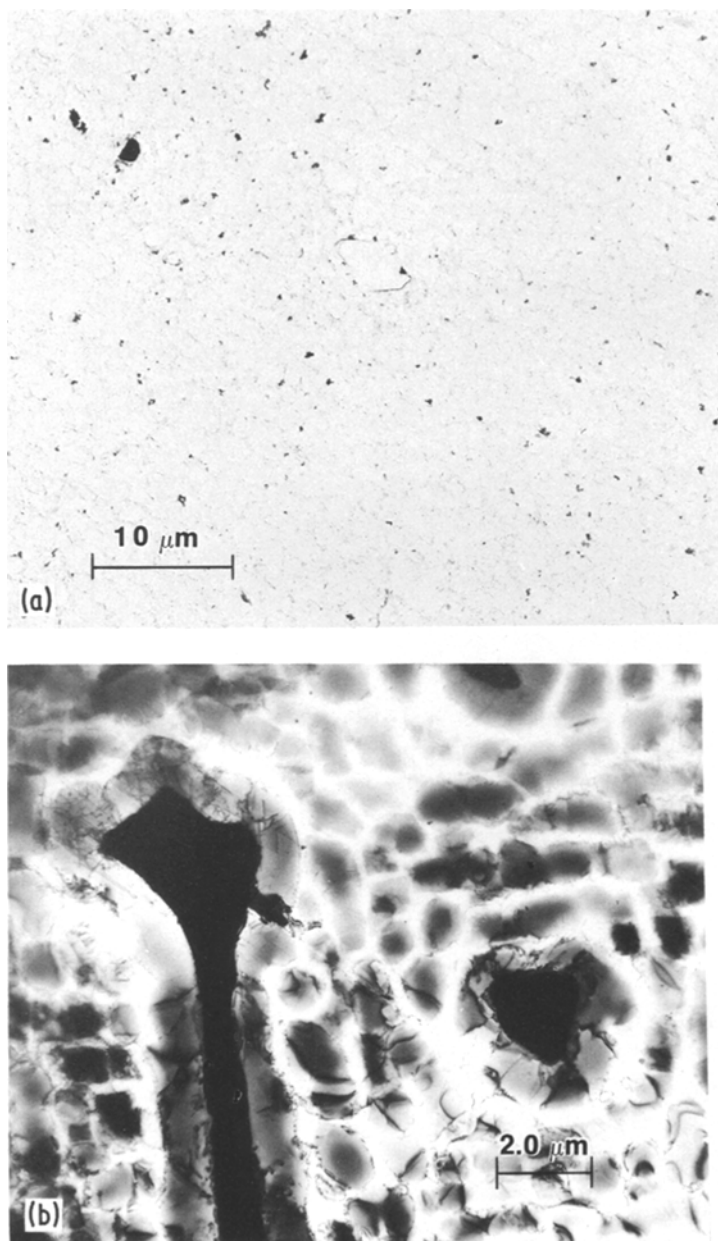


*Figure 10* Precipitation in the blade substrate are seen in a replica (a) with fairly even distribution. Large MC carbides in the thin foil (b) are often found to be surrounded by a  $\gamma'$  envelope.

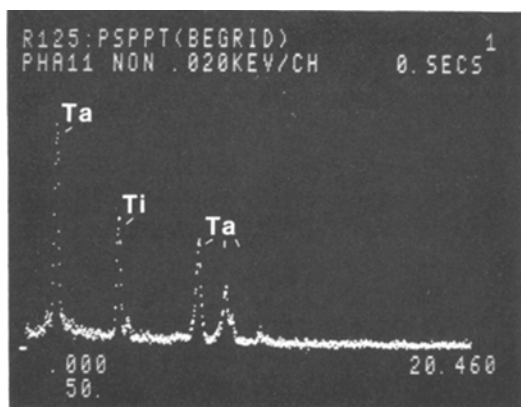


Figure 11 An EDS spectrum from a large precipitate in the coating containing Ta and Ti.

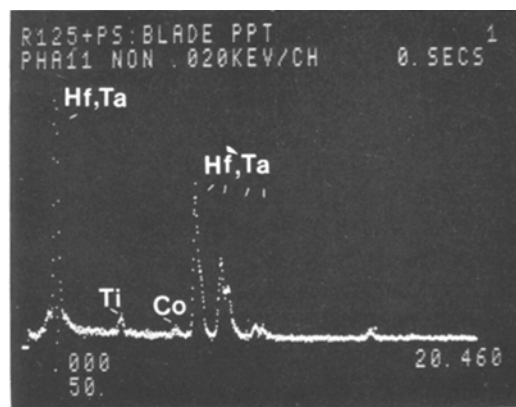


Figure 12 An EDS spectrum from a large precipitate in the blade containing Hf, Ta and a small amount of Ti.

strength of the matrix/precipitate bond. Grain sizes in the coating can be determined from the thin foil micrographs.

In the blade there appear to be no large aggregates of precipitates (Fig. 10a), and the precipitates are less numerous than in the coating, as expected from the Pt-shadowed replicas. Often these phases seem to be associated with eutectic areas. Very large precipitates, probably MC carbides, are seen in the blade. Transmission electron micrographs show that these phases are often surrounded by a  $\gamma'$  envelope (Fig. 10b).

Differences in composition between coating and blade precipitates were also observed. In the coating, EDS spectra show that the large precipitates are rich in Ta and Ti (Fig. 11). Selected-area electron diffraction patterns from these indicate that the phases are MC carbides, with a lattice parameter approximately that of either TiC or TaC (0.44 nm fcc). While one of the fine precipitates in the coating was found to be of the Ta-Ti type, most of the fine ones contain Hf and occasionally a small amount of Zr. These latter phases, then, are similar to those present at the interface. Precipitates in the blade seem to be different from those in the coating, with the large ones containing Hf and Ta, with some Ti and a very little Co (Fig. 12). This analysis is consistent with the phases being MC carbides. Two small blade precipitates were seen to be high in Al, and no other detectable element. These may be aluminium oxides, but no identification has been made. Statistics on the types of phases in the blade are poor, however, since fewer precipitates are present than in the coating.

#### 4. Conclusions

(1) The interface between a Rene' 125 plasma-sprayed coating and substrate Rene' 125 blade has been found by extraction replication to contain fine  $\text{HfO}_2$  precipitates, identified by a combination of selected-area electron diffraction and energy dispersive analysis.

(2) Examination of the Pt-shadowed replica shows small  $\gamma'$  dendrites, which are associated with the interface and lie primarily on the substrate side. These dendrites may indicate local melting of the substrate during spraying.

(3) Thin foil micrographs from an interfacial region confirm the identification of the dendrites as  $\gamma'$ , and show that all  $\gamma'$  precipitates in the melted areas have formed with the same orientation relative to the matrix.

(4) The coating is fine-grained, and somewhat inhomogeneous with regard to precipitate distribution. Large precipitates have been identified as MC carbides, where "M" is mainly Ti and Ta. Fine precipitates in the coating contain Hf and sometimes a little Zr. Examination of thin foils from the coatings shows that phases are present at many of the grain boundaries in the coating.

(5) Precipitates in the blade are not as numerous as in the coating, and are different in chemistry, with Hf and Ta predominating in the large phases. There are probably MC carbides, and often are surrounded by a  $\gamma'$  envelope.

(6) Each of the five methods of specimen preparation has its advantages, and the different but complementary data can be used to provide a better understanding of the microstructure.

## Acknowledgements

The authors would like to thank D. Rigney of our Aircraft Engine Business Group for supplying the coated blade and C. R. Rodd for the optical microscopy and metallographic preparation.

## References

1. L. W. MURR, "Electron Optical Applications in Materials Science" (McGraw Hill, New York, 1970) p. 170.
2. H. F. MERRICK, *Met. Trans.*, **4** (1973) 885.
3. J. M. LARSON, *ibid.* **7A** (1976) 1497.
4. H. J. BEATTIE, Jr and W. C. HAGEL, *Trans. AIME* **221** (1961) 28.
5. C. C. CLARK and J. S. IWANSKI, *ibid.* **215** (1959) 648.
6. S. KIHARA, J. B. NEWKIRK, A. OHTOMO and Y. SAIGA, *Met. Trans.* **11A** (1980) 1019.
7. K. C. ANTONY and J. F. RADAVIDICH, "Superalloys 1980" edited by J. K. Tien, S. T. Wlodek, H. Morrow, M. Gell, G. E. Maurer (ASM, Metals Park, Ohio, 1980) p. 257.
8. M. F. HENRY and N. S. STOLOFF, *J. Mater. Sci.* **7** (1972) 1477.
9. A. M. RITTER, "Microstructural Science", Vol. 5, edited by J. D. Braun, (Elsevier North-Holland, New York, 1976) p. 373.
10. R. J. SHEHER and G. N. MANIAR, *Metallogr.* **5** (1972) 409.
11. W. L. MANKINS, J. C. HOSIER and T. H. BASSFORD, *Met. Trans.* **5** (1974) 2579.
12. J. H. MOLL, G. N. MANIAR and D. R. MUZYKA, *ibid.* **2** (1971) 2143.
13. C. AUBIN, J. H. DAVIDSON and J. P. TROTTIER, "Superalloys 1980", edited by J. K. Tien, S. T. Wlodek, H. Morrow, M. Gell, G. R. Maurier (ASM, Metals Park, Ohio, 1980) p. 345.
14. A. M. RITTER and M. F. HENRY, *J. Mater. Sci.* **17** (1982) 79.
15. M. DAHLEN and H. FISCHMEISTER, "Superalloys 1980", edited by J. K. Tien, S. T. Wlodek, H. Morrow, M. Gell, G. W. Maurer (ASM, Metals Park, Ohio, 1980) p. 449.

Received 18 January  
and accepted 22 February 1982